

# Thermo-Physical Characteristics of Building Glass Wool Insulant: A Review of Experimental Results and Well-Adapted Techniques

**Laurent Marmoret**

University of Picardy (UPJV), Innovative Technology Laboratory (LTI), Civil Engineering Department (GC) of Institute of Technology of the University (IUT), Amiens, France

**Email address:**

Laurent.marmoret@u-picardie.fr

**To cite this article:**

Laurent Marmoret. Thermo-Physical Characteristics of Building Glass Wool Insulant: A Review of Experimental Results and Well-Adapted Techniques. *International Journal of Systems Engineering*. Vol. 1, No. 1, 2017, pp. 1-9. doi: 10.11648/j.ijse.20170101.11

**Received:** March 17, 2017; **Accepted:** April 5, 2017; **Published:** April 15, 2017

---

**Abstract:** There is need of experimental determination of thermo-physical properties of building materials to bridge the gap between theoretically prediction and real performance of buildings. Few references present structural, hydric and thermal properties of insulation materials in the same publication. This study aims to determine main thermo-physical characteristics of two glass wools. This publication wants also to review well-adapted experimental techniques because of their structural morphology. Inter-fiber space (pores) and fibers were studied by scanning electron microscope imaging (SEM) at the microscopic scale. The chemical composition of the fibers and binder will then be shown by coupling SEM to EDX detector. On macroscopic scale, the structural characteristics such as fiber diameter, the pore radius, total porosity, the surface area and the air permeability will be introduced. The hydraulic properties (such as sorption isotherm and vapor permeability) and thermal properties (conductivity and diffusivity) are then studied. Some influences between these thermo-physical parameters are presented. Relations between air permeability and humidity content against thermal will be analyzed.

**Keywords:** Building, Thermal Insulation, Glass Wool, Permeability, Thermal Conductivity

---

## 1. Introduction

Since the 1970s and the global energy crisis, building insulation production processes have evolved; Manufacturers seeking to improve the thermal properties of their products. Nowadays, experts have highlighted the warming of the earth planet. The building and construction sector can be considered a key sector for sustainable development: 30-40% of all primary energy is used in buildings [1] and, in terms of CO<sub>2</sub> emissions, buildings in the developed world contribute approximately 50% (27% from dwellings). The European Commission's recent package of proposals on climate and energy presents new aims for 2020 (compared to 1990, so called EU's 20-20-20): 20% less energy consumption, 20% of energy coming from Renewable Energy Source (RES), and reducing greenhouse gas (GHG) emission by 20%. Sufficient insulation is considered the most efficient factor to reduce heating energy in new and existing buildings. To achieve the EU's 20-20-20, European member states have imposed more stringent requirements in building codes.

Building energy consumption together with the environmental emissions during the manufacturing, production, transportation, using and recycling phases of insulation materials are studied in a life cycle perspective. However, these studies suffer from many sources of uncertainty, especially coming from the lack of experimental measurements on-site and on laboratory. Measurement is central to bridge the gap between theoretically predicted and real life performance of buildings. Although the main criterion for choosing an insulating material remains the thermal conductivity, thermal regulation French and European standardization introduce other criteria for health and environmental impact. In France, the certification so-called ACERMI determining fire resistance properties, mechanical, thermal, acoustic and moisture insulation materials to establish ISOLE classification. Certifications testing have been defined to the buyer and the setter in order to know the indications and contraindication during the implementation. They are therefore more interested in the consequences in terms of properties in use that from the

causes due to structural organization of the fiber medium.

To study the effect of structural organization, two glass wools have been selected. Structural, hydric and thermal characteristics have been determined experimentally. Glass wool was chosen because it represents the most widely used insulant on the world market. While glass wool is the subject of several publications in the literature, few of them present experimental thermo-physical properties [2]. Difficulties lie in the characterization of porous materials presenting important porosity (> 95%) with very large pores. Therefore the experimental equipment usually used for building materials like concrete, and plaster are not suitable.

The present work aims to present experimental structural, hydric and thermal characteristics of glass wool. Measurements of different techniques have been compared in order to establish their interest. This important work has been possible thanks to the contribution of French laboratories specialized either in textile materials characterizations or in finely divided porous materials characterization.

## 2. Materials and Methods

Two glass wools, denoted L1 and L2 in this presentation, were tested. They are usually employed for the insulation of building roofs. Samples were cut from panels of 60 x 125 x 10 cm (Fig. 1) supplied by the ISOVER company. Wools are composed of three components: fiber, air and binder.

### 2.1. Morphological Aspects

#### 2.1.1. Microstructural Analysis

The microscopy platform of University of Picardie Jules Verne (UPJV) has studied the morphology of these wools [3] at the microscopic scale. Samples were studied by scanning electron microscopy (SEM, Quanta 200 FEG SEM Environmental). The sample cell pressure was reduced to about 1 mbar for the study of single fibers and 0.28 mbar for studying binders and fibers. The structural heterogeneity and the random distribution of fibers were observed. Structural heterogeneity (Figure 2) relates both to the fiber geometry (length and diameter) and the pore size as well as the binder deposition.



Figure 1. Glass wool L1 (yellow) and L2 (green).

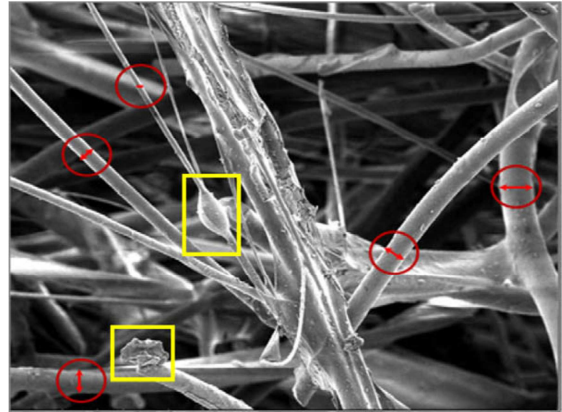


Figure 2. Heterogeneity of fiber (red circle) et binder in form of drop or clusters (yellow square)[2].

The SEM coupled to an EDX detector has determined the chemical composition of materials. Wool fiber (with or without binder) and the binder, in form of drop or clusters, have been studied.

#### 2.1.2. Macrostructural Analysis

The bulk density  $\rho_0$  may be determined using the following relationship:

$$\rho_0 = \varepsilon_s \rho_f = (1 - \varepsilon) \rho_f \quad (1)$$

where  $\varepsilon_s$  and  $\varepsilon$  represent the volume part respectively of solid only and of solid and gas (total porosity).  $\rho_f$  is the density of the glass fibers (from 2500 to 2800 kg. m<sup>-3</sup>, function of the type of fiber). To determine the total porosity, gravimetric is the most usual method. The sample is generally subjected to vacuum pressure before immersing it inside distilled water. The validity of this method can be discussed for the fibrous insulation. High porosity makes it impossible to keep water on and the presence of this water in the fibrous medium causes swelling of the structure.

A comparison of results from gravimetric (previous method) and helium pycnometer (more used in chemistry) has been undertaken. Pycnometric method requires knowledge of the true density ( $\rho_v$ ) of the material. The porosity is then calculated by the following equation:

$$\varepsilon = \frac{\rho_v - \rho_0}{\rho_v} \quad (2)$$

Samples are dried in an oven at a temperature of 40°C for 3 hours. The mass of the samples is obtained using a Mettler Toledo (LJ16). This balance enables also to check the water content of the materials. The bulk density  $\rho_0$  is calculated from the mass of a known volume of material. The true density  $\rho_v$  is determined by a helium pycnometer (AccuPyc 1330). Helium is an inert gas to the fibrous structure. Fibers are inserted into a cylindrical cell volume ( $V=10$  cm<sup>3</sup>). This volume is chosen in order to respect representative volume element (RVE) of material determined here primarily from the dimension of the fibers.

The specific surface area ( $S_v$ ) represents the degree of

division of the solid phase. It is one of the most important parameter to study the heat and mass transfer. An apparatus (ASAP 2020, Micromeritics) is used to monitor the absorption of a gas by the porous material. Several models can be also applied on sorption isotherm (BET, GAB,...) to deduce the specific surface area.

The intrinsic permeability of the material is determined from air permeability test (TEXTTEST FX 3300) [4]. In a previous work, we have observed dissolution of the binder has been observed due to the non-inert capacity of fiber material with water. So water permeability test can't be used [5]. Standard originally defined for textile fabrics (ISO 9237, 1995 F) has been followed to determine air permeability. Samples previously conditioned in an atmosphere of 20°C and 65% relative humidity are subjected to 200 Pa pressure gradient. Pressure gradient  $\Delta P$  (Pa) ranging from 1 to 2000 Pa is applied on a finite surface sample A (20 cm<sup>2</sup>) with thickness L (1 cm). When the flow  $q$  (m<sup>3</sup>·s<sup>-1</sup>) through the sample becomes constant, the air speed (ms<sup>-1</sup>) is calculated by:

$$U_D = \frac{q}{A} = k_A \cdot \frac{\Delta P}{L} = k_A \cdot i \quad (3)$$

The air permeability  $k_A$  (m·s<sup>-1</sup>) is measured in three directions as described in Figure 3.  $k_{A//1}$  and  $k_{A//2}$  are representative of the permeability in the direction of lamination of the layers of fibers ( $k_{A//1}$  being parallel to the fibers and  $k_{A//2}$  being perpendicular to the fibers).  $k_{A\perp}$  corresponds to the measurement in the perpendicular direction to the bedding plane and corresponds to the direction of heat flow in building use. The  $A_F$  anisotropic factor is determined by the ratio of air permeability in both directions:

$$AF = \frac{k_{A//1}}{k_{A\perp}} \quad (4)$$

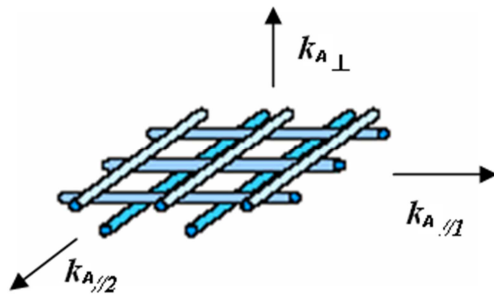


Figure 3. Air permeability and positioning bedding planes.

## 2.2. Hydric Characterization

Sorption isotherm [6] has been obtained by following the mass of initially dry 2.5 × 2.5 × 2.5 cm dimension samples placed in a desiccator with 21.5°C temperature and constant relative humidity defined by the used of saturated salt solution (Table 1). Equilibrium is established when samples are subjected to mass variation less than 0,001g. Once

equilibrium is reached, the present relative humidity is changed by higher percentage of relative humidity. The operation is repeated up to reach 100%, this is called adsorption process. The uncertainty on the relative humidity required by a salt is between 1 and 2%. Possible variations in partial pressure of water vapor at the interface solution/sample are considered negligible.

Table 1. Saturated salt solutions.

Saturated salt solution		Relative pressure (%) at 23°C
Potassium hydroxide	KOH	8
Sodium fluoride	NaF	57
Sodium chloride	NaCl	75
Potassium chloride	KCl	84
Potassium sulfate	K <sub>2</sub> SO <sub>4</sub>	97

The water vapor permeability is determined (Gintronic gravitest) following the A-Type status of NF EN ISO 12572. The NF EN ISO 12572 specifies the number of samples: at least five if the material surface exposed to the lower stream is less than 500 cm<sup>2</sup>, which is our case. A-Type condition corresponds to gradient pressure obtained with 0% humidity inside the cup (CaCl<sub>2</sub> salt) and 50% humidity in the chamber. The climatic chamber temperature is regulated at 23°C±2°C. The principle is to seal specimens at the top of the test cup containing a desiccant or a salt thereof to obtain a specific humidity at a temperature fixed on one side of the specimen. The other face is exposed to a moist atmosphere different from that inside the cup. The indoor humidity is always lower than the humidity of the room atmosphere. The device measures the mass change over time when the steam flow is constant. Depending on the parameters of temperature, humidity, pressure, mass change over time and the area of material exposed to the test, one can determine the equivalent air thickness  $S_d$  (m) and water vapor diffusion factor  $\mu$  (-) using the following equation for a thick material (m):

$$S_d = \mu d \quad (5)$$

In the liquid phase, a tensiometer (3S, GBX Instruments) is used [7] to establish the mass uptake kinetics. Thanks to this manipulation, the average pore radius using decane as the wetting fluid has been determined. The material initially dried, is weighed, suspended above the fluid in a closed chamber to reduce the exchange surface by convection. Few minutes are necessary before starting the test to establish thermo-hydric equilibrium between the material and the atmosphere of the room. The vessel containing the fluid is moved with the 100 μm·s<sup>-1</sup> maximum speed until it reaches a contact between the material and the fluid. Meniscus appears above the contact surface and after the fluid is absorbed inside the material due to capillary pressure. The total mass  $m_t$  (sample and liquid absorbed) is measured by the tensiometer balance (precision 10<sup>-4</sup> g) and a computer records sample mass every 0.2 s. Mass is composed of two components: firstly, the dampening mass due to the meniscus ( $m_w$ ) assumed to be constant during the test and secondly the mass of liquid absorbed in the material ( $m_a$ ). The total mass  $m_t$  is the sum of these two masses  $m_w$  and  $m_a$ :

$$m_t(t) = m_w + m_a(t) \quad (6)$$

Usually the duration of the test is between 100 and 600 seconds depending on the materials. The meniscus mass ( $m_w$ ) is assumed constant after 1 second. This mass is determined by subtracting final mass  $m_t$  (meniscus + absorbed fluid) with the mass without meniscus (absorbed fluid) when the fluid and the material are not in contact. Once the mass of the meniscus known, the mass of fluid absorbed by the material ( $m_a$ ) can then be determined as a function of time during the test. Relationships have been established to determine the kinetics of the average pore radius.

### 2.3. Thermal Characterization

Various thermal methods have been used to characterize materials depending on the objective. In the case of dry materials, thermal conductivity (or thermal resistance) has been determined by steady state techniques like guarded hot plate and heat flowmeter (HFM) techniques. In the case of moist materials, transient techniques are most appropriated because time test is short and flow is low. Thermal conductivity and thermal diffusivity can be simultaneously determined by transient plane source technique [6] in axial and radial directions of the probe. Standard test protocols have been followed. For example, ASTM C 518-98 American and European ISO Standards 8301 for the HFM and ISO 2007-2 method for Hot Disc method have been studied.

## 3. Results and Discussion

Glass fibers and a synthetic binder have been associated to produce glass wool. Scanning electron microscope (SEM) images show heterogeneity in fibers beds (Figure 2). Average fiber diameter has been estimated to 14  $\mu\text{m}$  (thick fibers) by statistical analysis. Glass fiber is produced by industrial process make it more regular than in the case of natural fiber. All glass belongs to the standard class type E. The binder appears in form of droplets or clusters attached on the fibers. Regular distribution has been observed with an average thickness of 500 nm. When SEM is coupled to the EDX

detector, same chemical composition (Figure 4) is obtained for glass fibers of wool L1 and L2 with significant presence of silicon (Si) and sodium (Na). Analysis of the binder reveals significant differences between the two wools (Figure 5). In particular the presence of Magnesium (Mg) for L1 and sulfide (S) for L2 can be observed. We conclude that differences in the chemical composition of the wool come essentially from binders.

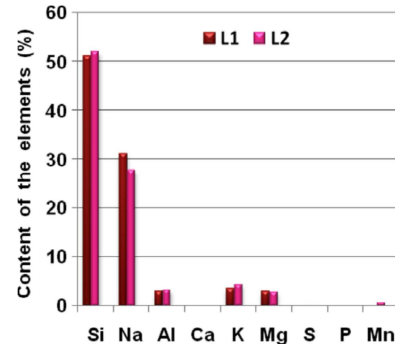


Figure 4. Chemical composition of wool fibers L1 and L2 [2].

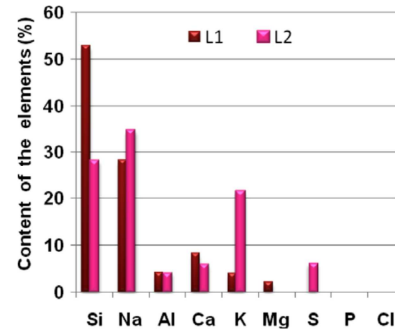


Figure 5. Chemical composition of wool binders L1 and L2 [2].

Total porosity of the wool L1 can be obtained by helium pycnometer measurement and gravimetric method. Good coherence between these methods can be observed (Table 2) taking into account accuracy. L2 wool presents a lower total porosity and a higher bulk density than L1. Due to density greater than 20  $\text{kg m}^{-3}$ , both wools like most building fibrous insulation are classified as heavy insulation.

Table 2. Densities and total porosity of glass wool.

Sample	Technique of measurement	Bulk density $\rho_0$ [ $\text{kg. m}^{-3}$ ]	True density $\rho$ [ $\text{kg. m}^{-3}$ ]	Total porosity $\epsilon$ [%]
L1 wool	pycnometer	68,6 $\pm$ 2,2	2620 $\pm$ 70	97,4 $\pm$ 1,1
L1 wool	gravimetric	79,0 $\pm$ 3,1		96,9 $\pm$ 1,8
L2 wool	gravimetric	119,0 $\pm$ 2,9		95,4 $\pm$ 1,6

The specific surface area is determined experimentally by a specific equipment (ASAP 2020, Micromeritics). Material is brought into contact with measuring cell containing krypton gas. Krypton is selected in order to be inert against fibrous medium. In the case of low gas contents (<0.35-0.40), molecules of krypton is strongly adsorbed in a monomolecular layer. By applying the BET method, the specific surface area is obtained. This value is important for L1 wool ( $S_v = 0.2332 \pm 0.0120 \text{ m}^2. \text{g}^{-1}$ ) showing that the medium is finely divided. However, we find that the

coefficient C determined by the BET method is high. We conclude that krypton molecule may not be the most suitable. Using the assumption of an equivalent insulating medium consisting of fibers of the same diameter ( $D_f$ ) having the same surface area, it is possible to define the average fiber diameter from the usual equation:  $D_f = 4/S_v$ . Fiber diameter can be extracted from this equation to  $7.2 \pm 0.5 \mu\text{m}$ . Compared to value obtained by SEM images statistical analysis ( $14 \pm 6 \mu\text{m}$ ) an important difference is obtained. Considering that industrial process make identical fiber

diameter, only ten fibers are selected for statistical analysis. But manufacturer has confirmed the use of recycled fiber of various diameters that confirm the need of using more than 10 fibers for statistical analysis and can explain the difference.

Tensiometer has been used to determine pore radius. Porous media are generally considered equivalent to cylindrical multiple capillaries although this simplistic representation is not representative of real porous fibrous network. Most of laws are established based on this assumption. Washburn, Laplace and Jurin laws have been used to determine fluid speed and its path inside the porous network. During infiltration period, viscous forces are more important in the fine pores than in coarse pores. Fine pores control the infiltration rate while coarse pores act as a storage area. Mean radius of fine pores (Table 3) can be determined by Washburn Law ( $R_w$ ) although mean radius of coarse pores

is obtained by Laplace law ( $R_L$ ) and a hydraulic radius ( $R_v$ ) usually used in fluid transfer can be calculated by  $R_v = \sqrt{R_w R_L}$ .

Table 3. Pore Radius.

	$R_w$ ( $\mu\text{m}$ )	$R_L$ ( $\mu\text{m}$ )	$R_v$ ( $\mu\text{m}$ )
L1 wool	9,6	252,9	49,3
L2 wool	6,9	203,7	37,5

We have determined the air permeability by using five samples of L1 and L2 wools. Results are presented in Figures 6 and 7 with respect of 5% uncertainty defined in standard ISO 9237. We have performed air permeability in three directions of the medium defined according to figure 3. As linear relationship is observed between air speed and pressure gradient, Darcy's law can be applied.

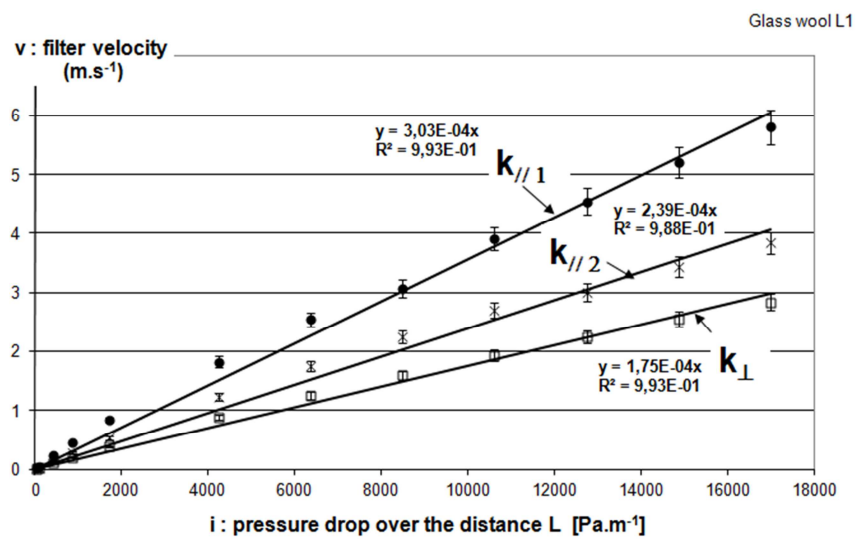


Figure 6. Glass wool L1 air permeability.

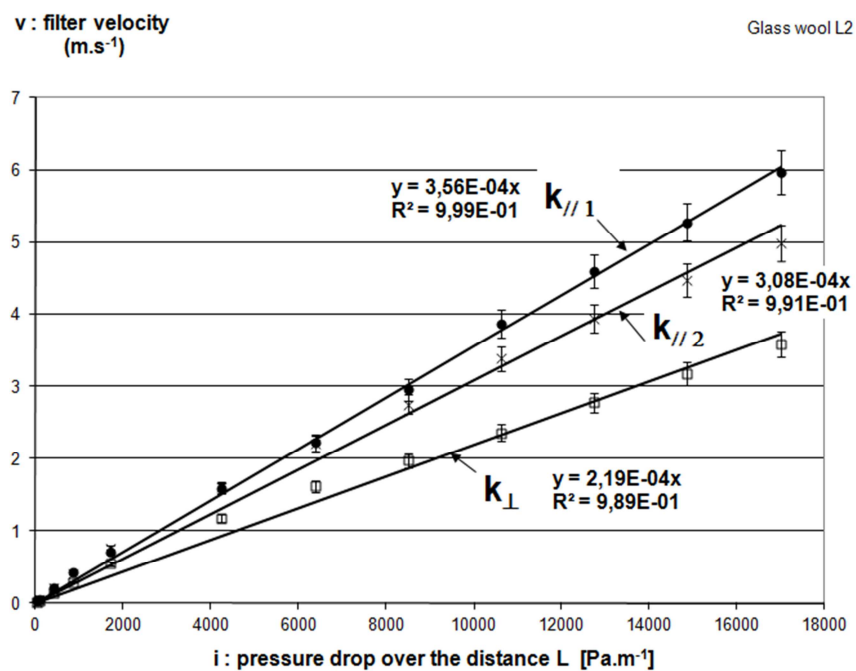


Figure 7. Glass wool L2 air permeability.

Table 4 presents air permeability values for L1 and L2. Air permeability is more important for L2 whatever the direction of the flow (perpendicular or parallel). This remark is coherent with porosity values. For a given material, the air permeability is lowest in the direction perpendicular to the stratification (i.e. in the effective direction of use of the glass wool) and highest in the flow directions parallel to the stratification plane. The highest value being measured in the direction along the fiber length ( $k_{A//1}$ ). A large difference is observed between  $k_{A//1}$  and  $k_{A//2}$ , even if it is generally admitted they are usually equivalent. An anisotropy factor ( $A_F$ ) of 2 is usually observed in common glass wools. In the case of our materials, lower  $A_F$  values are obtained, ranging from 1.37 to 1.73 (Table 4). These lower values can be assigned to the “crimping” industrial process described by the manufacturer [9]. The intrinsic permeability ( $k$ , in  $m^2$ ) is calculated from the air permeability  $k_A$  using the following equation:

$$k = K_a \cdot \frac{\eta}{\rho \cdot g} \quad (7)$$

Where  $\eta$  is the dynamic viscosity ( $1.81 \cdot 10^{-5}$  Pa.s),  $\rho$  the density of air ( $1.2 \text{ kg} \cdot m^{-3}$ ) and  $g$  is the acceleration due to gravity ( $9.81 \text{ m} \cdot s^{-2}$ ). The results are presented in Table 4.

**Table 4.** Intrinsic permeabilities ( $k$ ) and anisotropic factor ( $A_F$ ).

	Glass wool L1	Glass wool L2
$k_{//1}$ ( $m^2$ )	$4.66 \cdot 10^{-10}$	$5.47 \cdot 10^{-10}$
$k_{//2}$ ( $m^2$ )	$3.67 \cdot 10^{-10}$	$4.73 \cdot 10^{-10}$
$k_{\perp}$ ( $m^2$ )	$2.69 \cdot 10^{-10}$	$3.36 \cdot 10^{-10}$
$A_{F1} = \frac{k_{A//1}}{k_{A\perp}}$	1.73	1.62
$A_{F2} = \frac{k_{A//2}}{k_{A\perp}}$	1.37	1.40

Pressure gradient data due to the flow of a single phase fluid through a glass wool bed are relatively scarce in the

literature. We can notice the work of Jackson et al. [10]. They have reported data from different investigators in the form of a non-dimensional term ( $k/R_f^2$ ) as a function of solid volume fraction ( $\phi=1-\epsilon$ ) where  $R_f$  is fiber radius. Coherent values can be observed with our results.

The measurements [11] of adsorption isotherms were performed in laboratory conditions at  $23 \pm 1^\circ\text{C}$ . The samples were placed in desiccators with different solutions (table 1) to simulate different values of relative pressures. The initial state was dry material ( $m_o$ ) after maintained samples in an oven at  $80^\circ\text{C}$ . The mass of samples was measured until the steady state value of the mass was achieved ( $m_w$ ). Then, the equilibrium moisture content by mass ( $\omega$  in  $\text{kg} \cdot \text{kg}^{-1}$ ) was calculated according by gravimetric method:

$$\omega = \frac{m_w - m_o}{m_o} \quad (8)$$

The volumetric water content ( $\theta$ ) can be calculated with  $\theta_l = (\rho_l / \rho_o) \cdot \omega$  where  $\rho_l$  and  $\rho_o$  are densities of water and material respectively. The experimental results on the equilibrium volumetric moisture content against relative pressures are given in Figure 8. According to IUPAC classification [9], these sorption curves are classified as type II. This type corresponds to non-porous or macroporous media. The curves obtained for the two wools are quite the same but we notice that L1 is a little more hygroscopic than L2. Three clearly defined regions can be distinguished. For  $0 < \phi < 0.8$ , in the adsorptionally bound moisture region (with mono on the part ① and multi-molecular layer on part ②), the amount of water adsorbed is very small. Volumetric water content doesn't exceed 0.1. In the capillary bound moisture region ( $\phi > 0.8$ ), the increase of volumetric water content is important. For example, at  $\phi=0.90$ , volumetric moisture content is 0.30 for L2 and 0.34 for L1. The water content difference cannot be only assigned to the experimental error [12] which doesn't exceed 5%.

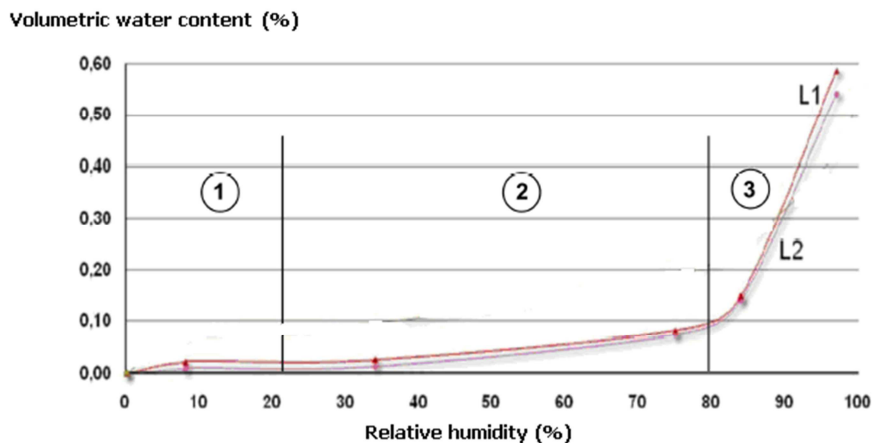


**Figure 8.** Sorption isotherm for glass wool (L1 and L2) [2].

Vapor permeability is carried on 5 samples of 18 mm thick L1 glass wool. The material is sealed above the test cup containing either a saturated aqueous solution or a desiccant.

All is placed in a test chamber regulated in temperature and humidity inside the vapor permeability-meter. Tests are performed in dry cup method with  $23^\circ\text{C}$  temperature and

relative humidity gradient obtained with  $0 \pm 3\%$  on the dried surface and  $50 \pm 3\%$  on the other face (condition A of the standard). The test cup dry informs on the low moisture materials performance when moisture transfer is dominated by vapor diffusion. Measurement results are summarized in Table 5. It should be noted that due to the definition of the equivalent thickness of air  $S_d$  (m), when  $S_d$  is low then water vapor permeability is high. Compared with different materials such as vapor barrier ( $S_d \geq 18$  m) or OSB3 panel of 15 mm thickness ( $S_d: 3.2$  m), the air thickness  $S_d$  for L1 wool

is very low and therefore the vapor permeability is very high. Using the definitions and  $S_d$  of vapor diffusion factor  $\mu$  water (see § II. 3), it is possible to determine the permeability to water vapor wool:  $\pi_v = 5.84 \cdot 10^{-11} \text{ kg.Pa}^{-1}.\text{m}^{-1}.\text{s}^{-1}$ . This value can be compared to the concrete ( $\pi_v = 6.24 \cdot 10^{-12} \text{ kg.Pa}^{-1}.\text{m}^{-1}.\text{s}^{-1}$ ). It should be noted that in literature, wool permeability is considered equal to  $\pi_v = 1.5 \cdot 10^{-10} \text{ kg.Pa}^{-1}.\text{m}^{-1}.\text{s}^{-1}$  two times lower than our value. This difference can be assigned to treatments introduced during the crimping process [9].

Table 5. Air thickness for L1 wool.

Sample	Mean temperature (°C)	Mean Humidity (%)	Air speed (m/s)	Atmospheric pressure (mbar)	mass speed coefficient ( $\text{g}.\text{m}^2.\text{24h}^{-1}$ )	Air Thickness $S_d$ (m)	Deviance Ecart-type $S_d$ (m)
Laine L1	23,0 ±0,5	50,0 ±3	0,3	1011,18	348,64	0,057	0,002

According to ISO 8302, guarded hot plate (GHP) has been used to determine thermal conductivity of glass wool L1 against sample mean temperature (Figure 9). Dimension of the sample is 246 x 250 x 60mm. About 6 hours are necessary to achieve the temperature difference of  $10^\circ\text{C}$  between the two external surfaces of the sample as required by the ISO 8302 standard. This equilibrium is obtained by using 0.4 W thermal power. This procedure is repeated for successive mean sample temperatures of 10, 20, 30 and  $40^\circ\text{C}$ . At the temperature of  $10^\circ\text{C}$  (standard value), thermal conductivity is:  $\lambda = 0.0369 \pm 0.0007 \text{ W}.\text{(m.K)}^{-1}$ . Variation of thermal conductivity ( $\lambda$ ) against sample mean temperature (MT) shows linear curve defined as  $\lambda = 0.03443 + 0.000244 \cdot \text{MT}$  (R-squared: 99.28%). Measurement error of 7% is recommended by ISO 8302 standard. Error bars have been reported in figure 9 as well as HFM and Hot Disc experimental values. Bulk anisotropic module has been used to determine thermal conductivity and thermal diffusivity in axial and radial directions (figure 10 and table 6). Axial conductivity ( $\lambda_a$ ) is referred to as through-plane in sample perpendicularly of the thermal probe (figure 10). In our case, axial conductivity is in the same direction of  $k_{A/1}$  and  $k_{A/2}$  (figure 3). Radial conductivity ( $\lambda_r$ ) is referred to as in-plane in sample (similar direction in the sample to  $k_{A\perp}$  in figure 3) and corresponds to the direction of heat flow in building use. That is the reason of a good coherence can be

observed excepted for results from Guarded hot plate, High flowmeter and Hot Disc in radial direction but not with results from Hot disc in axial direction. Industrial process for making glass wool promotes thermal flow only in building use direction.

Another interesting point is the ratio axial conductivity against radial conductivity is equal to 1.32 in the dry state. This value is close to anisotropic factor defined in table 4. We can notice than the same ratio is obtained for diffusivity (equal to 1.32 too). These remarks confirm thermal conduction and diffusion are mainly sent through the pores by the air inside pores [13].

To study the effect of humidity content on thermal characteristics, Hot Disc method seems to be the most interesting technique [14]. A very low flow (20mW) is applied during a short time (less than 200 s) in order to create the lowest influence on humidity content [15]. The Hot Disc probe is a disc of 30 cm diameter so that respect the characteristic time. A volume of sample around the probe defined by the probing depth is submitted to the flow. Cylindrical samples of 10cm diameter and 10cm length has been prepared. Before being placed in a climatic chamber, samples are dried until stabilized mass. Climatic chamber has been regulated at 50%, 85% and 95% and  $25^\circ\text{C}$  temperature. Samples are maintained in climatic chamber during 8 days (stabilized mass) before being tested.

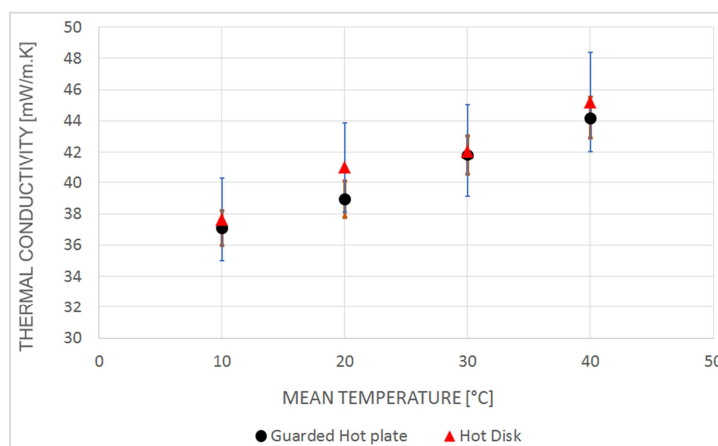


Figure 9. Comparison Thermal conductivity results using GHP, HFM and Hot Disc methods.

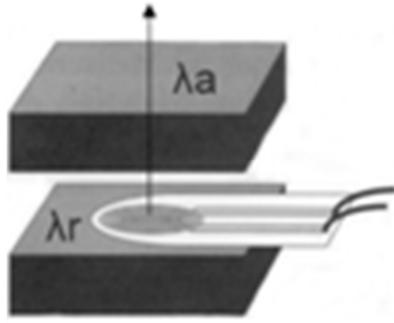


Figure 10. Axial and radial direction in Hot Disc method.

To check the validity of thermal diffusivity experimental value, specific heat capacity has been determined by DSC technique. Considering density defined in table 2, it is possible to calculate thermal diffusivity from specific heat capacity. Calculated diffusivity value from DSC technique is  $0.65\text{mm}^2.\text{s}^{-1}$ . This value is coherent with diffusivity determined in radial direction by Hot Disc method. We can also notice that conductivity and diffusivity increased highly for 95% compared to 50% and 85%. Sorption isotherm graph (figure 8) confirm this remark showing the influence of humidity on moisture content starts from 35% but the increase is very most important from 85%. Thermal conductivity and diffusivity present surprising values for 85% by Hot Disc in radial direction.

Table 6. Thermal conductivity and diffusivity against humidity.

	thermal conductivity $\text{W}.\text{(m.K)}^{-1}$		Thermal diffusivity $\text{mm}^2.\text{s}^{-1}$	
	Axial	Radial	Axial	Radial
Dry sample	0.0529	0.0404	0.906	0.687
50% HR	0.1155	0.0413	2.105	0.759
85%HR	0.1266	0.0383	2.304	0.697
95% HR	0.1686	0.0513	3.065	0.934

## 4. Conclusion

Main thermo-physical characteristics of two glass wools (so called L1 and L2) have been presented. Crosscheck between structural, hydric and thermal properties has been also realized to check the validity of experimental results. Mean fiber diameter has been determined by statistical image analysis and indirectly calculated from specific area measurement. Usually glass fibers are produced by industrial process so diameter is regular but these wools are composed by recycled fiber of different diameters. Glass wool is also composed of binder which can pull out when water permeability or capillary imbibition tests has been done. Air permeability seems to be the most representative test to determine intrinsic permeability. Glass wool vapor permeability test confirms the necessity of adding vapor retarder as soon as vapor pressure gradient is important. Air permeability and sorption isotherm curve results are coherent with thermal properties values. Thermal conductivity and diffusivity present important increased for 95% but not for 50

and 85%. Anisotropic factor determined from air permeability tests in 3 directions are also coherent with ratio of thermal conductivity and of thermal diffusivity values in axial and radial directions of the probe.

## References

- [1] Building and climate change, United Nations Environment Programme, ISBN: 978-92-807-2795-1, 2007.
- [2] F. Achchaq, Caractérisation hygrothermique de matériaux fibreux isolant, UPJV thesis, 2008.
- [3] F. Achchaq, K. Djellab, H. Béji, L. Marmoret, Hydric, morphological and thermo-physical characterization of glass wools: From macroscopic to microscopic approach, Construction and Building Materials, 23, pp 3214–321, 2009.
- [4] L. Marmoret, M. Lewandowski, A. Perwuelz, An Air Permeability Study of Anisotropic Glass Wool Fibrous Products, Transport in Porous Media, ISSN 0169-3913, Vol. 86, N°2, 2012.
- [5] L. Marmoret, H. Beji, M. Lewandowski, A. Perwuelz, Using capillarity and permeability experimental data to study the flow phenomena inside a fibrous medium, Book title: Focus on porous media research, Chapter ID: 13741, Nova Science publishers (NY, USA), Jan 2013.
- [6] L. Marmoret, F. Collet, H. Beji, Moisture adsorption of glass wool products, High Temperature High Pressure, Vol. 40, N°1, pp. 31–46, Old City Publishing Inc, 2011.
- [7] L. Marmoret, H. Beji, A. Perwuelz, Determination of the pore sizes and their influence on the dynamics of imbibition into thermal insulating glass wool, Defect and Diffusion Forum, Vols. 312-315 pp 812-817, 2011.
- [8] A. Maqsood, M. Anis-ur-Rehman, Transient plane source (tps) sensors for simultaneous measurements of thermal conductivity and thermal diffusivity of insulators, fluids and conductors, Materials Science and Engineering, Volume 51, 2013.
- [9] S. Bergonnier, F. Hild, J. B. Rieunier, S. Roux; Strain hétérogénéités et local anisotropy in crimped glass wool, Journal of Material Science, N°40, pp 5949–5954, 2005.
- [10] G. W. Jackson, D. F. James, The permeability of fibrous porous media, the Canadian journal of chemical engineering,, volume 64, 1986.
- [11] International Union of Pure and Applied Chemistry, Reporting physisorption data for Gas/solid systems with special reference to the determination of surface area and porosity, Pure and Applied Chemistry, Vol. 57, N°4, pp 603-619, 1986.
- [12] P. Schneider, Adsorption isotherm of microporous-mesoporous solids revisited, Applied Catalysis A: General, 129, pp 157-165, 1995.
- [13] L. Marmoret, H. Humaish, A. Perwuelz, H. Béji, Anisotropic structure of glass wool determined by air permeability and thermal conductivity measurements, Journal of Surface Engineered Materials and Advanced Technology, Vol. 6, pp 72-79, 2016.

- [14] H Humaish, L Marmoret, C Pelegris, H Béji, Effect of “crimped” glass wool structure on effective thermal conductivity, High Temperature High Pressure, High Temperature High Pressure, Vol. 45, 213-223, 2016.
- [15] L Marmoret, Assessment of hydrothermal performance by thermophysical characterization of a crimped glass wool building insulation, Journal of Building Physics, pp 1-16, Sage Publishing, 2016.